

Analytical results on channel capacity in uncompensated optical links with coherent detection

*Original*

Analytical results on channel capacity in uncompensated optical links with coherent detection / Bosco, Gabriella; Poggiolini, Pierluigi; Carena, Andrea; Curri, Vittorio; Forghieri, F.. - In: OPTICS EXPRESS. - ISSN 1094-4087. - ELETTRONICO. - 19:26(2011), pp. B440-B451. [10.1364/OE.19.00B440]

*Availability:*

This version is available at: 11583/2465783 since:

*Publisher:*

Optical Society of America (OSA)

*Published*

DOI:10.1364/OE.19.00B440

*Terms of use:*

This article is made available under terms and conditions as specified in the corresponding bibliographic description in the repository

*Publisher copyright*

(Article begins on next page)

# Analytical results on channel capacity in uncompensated optical links with coherent detection

G. Bosco,<sup>1,\*</sup> P. Poggiolini,<sup>1</sup> A. Carena,<sup>1</sup> V. Curri,<sup>1</sup> and F. Forghieri<sup>2</sup>

<sup>1</sup> Dipartimento di Elettronica, Politecnico di Torino, Corso Duca degli Abruzzi, 24 - 10129 Torino, Italy

<sup>2</sup> Cisco Photonics Italy srl, via Philips, 12 - 20900 Monza, Italy

\* [gabriella.bosco@polito.it](mailto:gabriella.bosco@polito.it)

**Abstract:** Based on a recently introduced model of non-linear propagation, we propose analytical formulas for the capacity limit of polarization-multiplexed ultra-dense WDM uncompensated coherent optical systems at the Nyquist limit, assuming both lumped and ideally distributed amplification. According to these formulas, capacity fundamentally depends on the transmitted power spectral density and on the total optical WDM bandwidth, whereas it does not depend on symbol-rate. Also, capacity approximately decreases by 2 [bit/s/Hz] for every doubling of link length. We show examples of capacity calculations for specific ultra-long-haul links with different polarization-multiplexed (PM) constellations, i.e. ideal PM-Gaussian, PM-QPSK (quadrature-phase shift keying) and PM-QAM (quadrature amplitude modulation). We show that the launch power maximizing capacity is independent of link length and modulation format. We also discuss the usable range of PM-QAM systems and validate analysis with simulations.

© 2011 Optical Society of America

**OCIS codes:** (060.1660) Coherent communications; (060.2330) Fiber optics communications; (060.2360) Fiber optics links and subsystems; (060.4080) Modulation.

---

## References and links

1. A. H. Gnauck, P. J. Winzer, S. Chandrasekhar, X. Liu, B. Zhu and, D. W. Peckham, "Spectrally efficient long-haul WDM transmission using 224-Gb/s polarization-multiplexed 16-QAM," *J. Lightw. Technol.* **29**, 373-377 (2011).
2. K. Schuh, F. Buchali, D. Roesener, E. Lach, O. Bertran-Pardo, J. Renaudier, G. Charlet, H. Mardoyan, and P. Tran, "15.4 Tb/s transmission over 2400 km using polarization multiplexed 32-Gbaud 16-QAM modulation and coherent detection comprising digital signal processing," *Proc. European Conference on Optical Communication* (2011), paper We.8.B.4.
3. A. Sano, T. Kobayashi, A. Matsuura, S. Yamamoto, S. Yamanaka, E. Yoshida, Y. Miyamoto, M. Matsui, M. Mizoguchi, and T. Mizuno, "100x120 Gb/s PDM 64 QAM transmission over 160 km using linewidth-tolerant pilotless digital coherent detection," *Proc. European Conference on Optical Communication* (2010), paper PD2.2.
4. T. Kobayashi, A. Sano, A. Matsuura, M. Yoshida, T. Sakano, H. Kubota, and Y. Miyamoto, K. Ishihara, M. Mizoguchi, M. Nagatani, "45.2Tb/s C-band WDM transmission over 240km using 538Gb/s PDM-64QAM single carrier FDM signal with digital pilot tone," *Proc. European Conference on Optical Communication* (2011), PD paper Th.13.C.6
5. J.-X. Cai, Y. Cai, C. Davidson, A. Lucero, H. Zhang, D. Foursa, O. Sinkin, W. Patterson, A. Pilipetskii, G. Mohs, and N. Bergano, "20 Tbit/s capacity transmission over 6,860 km," *Proc. Optical Fiber Communication Conference* (2011), paper PDPB4.

6. E. Torrenco, R. Cigliutti, G. Bosco, G. Gavioli, A. Alaimo, A. Carena, V. Curri, F. Forghieri, S. Piciaccia, M. Belmonte, A. Brinciotti, A. La Porta, S. Abrate, and P. Poggiolini, "Transoceanic PM-QPSK Terabit superchannel transmission experiments at baud-rate subcarrier spacing," *Proc. European Conference on Optical Communication* (2010), paper We.7.C.2.
7. P. P. Mitra and J. B. Stark, "Nonlinear limits to the information capacity of optical fibre communications," *Nature* **411**, 1027-1030 (2001).
8. J. Tang, "A comparison study of the Shannon channel capacity of various nonlinear optical fibers," *J. Lightw. Technol.* **24**, 2070-2075 (2006).
9. M. H. Taghavi, "On the multiuser capacity of WDM in a nonlinear optical fiber: coherent communication," *IEEE Trans. Inf. Theory* **52**, 5008-5022 (2006).
10. H. Haunstein and M. Mayrock, "OFDM spectral efficiency limits from fiber and system non-linearities," *Proc. Optical Fiber Communication Conference* (2010), paper OThM7.
11. A. D. Ellis, J. Zhao, and D. Cotter, "Approaching the non-linear Shannon limit," *J. Lightwave Technol.* **28**, 423-433 (2010).
12. R.-J. Essiambre, G. Kramer, P. J. Winzer, G. J. Foschini, and B. Goebel, "Capacity limits of optical fiber networks," *J. Lightwave Technol.* **28**, 662-701 (2010).
13. P. Poggiolini, A. Carena, V. Curri, G. Bosco, and F. Forghieri, "Analytical modeling of non-linear propagation in uncompensated optical transmission links," *IEEE Photon. Technol. Lett.* **23**, 742-744 (2011).
14. P. Poggiolini, G. Bosco, A. Carena, V. Curri, and F. Forghieri, "A simple and accurate model for non-linear propagation effects in uncompensated coherent transmission links," *Proc. International Conference on Transparent Optical Networks* (2011), paper We.B1.3.
15. A. Carena, V. Curri, G. Bosco, P. Poggiolini, and F. Forghieri, "Modeling of the impact of non-linear propagation effects in uncompensated optical coherent transmission links," submitted to *IEEE J. Lightwave Technol.*
16. M. Nazarathy, J. Khurgin, R. Weidenfeld, Y. Meiman, P. Cho, R. Noe, I. Shpantzer, and V. Karagodsky, "Phased-array cancellation of nonlinear FWM in coherent OFDM dispersive multi-span links," *Opt. Express* **15**, 15777-15810 (2008).
17. B. Goebel, B. Fesl, L.D. Coelho, and N. Hanik, "On the effect of FWM in coherent optical OFDM systems," *Proc. Optical Fiber Communication Conference* (2008), paper JWA58.
18. X. Chen and W. Shieh "Closed-form expressions for nonlinear transmission performance of densely spaced coherent optical OFDM systems," *Opt. Express* **18**, 19039-19054 (2010).
19. H. Louchet, A. Hodzic, and K. Petermann, "Analytical model for the performance evaluation of DWDM transmission systems," *IEEE Photon. Technol. Lett.* **15**, 1219-1221 (2003).
20. E. Torrenco, R. Cigliutti, G. Bosco, A. Carena, V. Curri, P. Poggiolini, A. Nespola, D. Zeolla and F. Forghieri, "Experimental validation of an analytical model for nonlinear propagation in uncompensated optical links," *Proc. European Conference on Optical Communication* (2011), paper We.7.B.2.
21. S. Benedetto and E. Biglieri, *Principles of digital transmission: with wireless applications* (New York: Kluwer, 1999).
22. G. Bosco, P. Poggiolini, A. Carena, V. Curri, and F. Forghieri, "Analytical results on channel capacity in uncompensated optical links with coherent detection," *Proc. European Conference on Optical Communication* (2011), paper We.7.B.3.
23. A. Carena, G. Bosco, V. Curri, P. Poggiolini, M. Tapia Taiba, and F. Forghieri, "Statistical characterization of PM-QPSK signals after propagation in uncompensated fiber links," *Proc. European Conference on Optical Communication* (2010), paper P4.07.
24. F. Vacondio, C. Simonneau, L. Lorcy, J.-C. Antona, A. Bononi, and S. Bigo, "Experimental characterization of Gaussian-distributed nonlinear distortions," *Proc. European Conference on Optical Communication* (2011), paper We.7.B.1.
25. C. E. Shannon, "A mathematical theory of communication," *Bell Syst. Tech. J.* **27**, 379-423 (1948).
26. G. Bosco, A. Carena, R. Cigliutti, V. Curri, P. Poggiolini, and F. Forghieri, "Performance prediction for WDM PM-QPSK transmission over uncompensated links," *Proc. Optical Fiber Communication Conference* (2011), paper OThO7.
27. A. Bononi and E. Grellier, "Quality parameter for coherent transmissions with Gaussian-distributed nonlinear noise," *Opt. Express* **19**, 12781-12788 (2011).

---

## 1. Introduction

Thanks to the revolutionary breakthrough in the field of optical fiber transmission introduced by coherent detection, the last few years have been characterized by an escalation of new records in terms of transmission distance, spectral efficiency (SE) and/or total capacity. This has been made possible by the use of high-order constellations and/or advanced spectral shaping techniques [1–6], together with distributed amplification and new generation fibers. How far this

process can be pushed depends on the actual ultimate performance limits of optical fiber transmission.

In this scenario, the accurate evaluation of the ultimate capacity of the optical channel has recently emerged as a topic of great interest to the community [7–12]. In particular, [12] provides accurate semi-analytical capacity estimates assuming single-polarization and non-linear compensation through backward-propagation. An important related topic is the optimal choice of modulation format vs. link characteristics, so that the actual practically obtainable capacity is maximized.

Here we address these topics using the model shown in [13–15] of the impact of non-linear propagation in coherent uncompensated transmission (UT) links with both distributed and lumped amplification. Such model is based on a frequency-discrete perturbative approach similar to that used in [16–18] for OFDM, adapted for serial transmission. Some of its analytical results also bear substantial similarity to those in [8], [19], which were obtained using a different perturbative approach, based on Volterra-series. Very good model accuracy was found through extensive simulations both with PM-QPSK at the Nyquist limit [13] (that is at symbol-rate channel spacing with rectangular spectra) and at wider channel spacings with various PM-QAM formats [14, 15]. A first experimental validation has been shown in [20].

Using this model and assuming the optimal Gaussian constellation [21], we first write a closed-form expression of the maximum optical channel capacity at the Nyquist limit for systems employing either distributed or EDFA amplification. We then assess the capacity of realistic hard and soft-decision PM-QAM formats, showing a few examples of application of the capacity formulas. We also assess the capacity of hard-decision PM-QAM formats at larger than symbol-rate frequency spacings and with non-rectangular spectra, resorting to the integral formula for the impact of non-linearity provided in [14, 15]. In this case, we validate the capacity results through a comparison with numerical simulations.

Preliminary results have been presented in [22], assuming terrestrial links, span length of 100 km with EDFA amplification and a hard-decision receiver. In this paper we further elaborate the capacity formulas and extend them to the cases of distributed amplification and soft-decision. We also add some performance results over submarine links (span length equal to 50 km).

This paper is structured as follows: in Sect. 2 we recall relevant results from [13–15], and extend them as needed. In Sect. 3 we derive the capacity limits for the case of lumped and ideally distributed amplification and point out certain key properties of such expressions. In Sect. 4 we discuss how to calculate the capacity of specific transmission formats, such as polarization-multiplexed (PM) quadrature phase-shift-keying (PM-QPSK) and PM quadrature-amplitude-modulation (PM-QAM). In Sect. 5 we provide a few examples, discussing key aspects of capacity optimization and identify the optimal usability distance ranges for various practical formats, highlighting BER-capacity relationships and ideal FEC requirements. Finally, we draw some conclusions.

## 2. Non-linear interference modeling

Our results are based on the theory introduced in [13–15], which is in turn based, to a significant extent, on a specific property of UT: the statistical distribution of each of the received constellation points, after digital signal processing (DSP), is approximately Gaussian, with independent components, even in the absence of added amplified-spontaneous-emission (ASE) noise in the link [23], [24]. In other words, it appears that the overall effect of non-linear propagation could be approximately modeled as excess additive Gaussian noise, at least for low-to-moderate non-linearity. We call this excess noise *non-linear interference* (NLI).

Based on this assumption, the system bit error rate (BER) then depends on a generalized

OSNR, defined so as to include NLI noise as follows:

$$\text{OSNR}_{\text{NL}} = \frac{P_{\text{Tx,ch}}}{P_{\text{ASE}} + P_{\text{NLI}}} \quad (1)$$

where  $P_{\text{Tx,ch}}$  is the average per-channel power and  $P_{\text{ASE}}$  is the dual-polarization ASE noise power within the OSNR noise bandwidth  $B_n$ . The NLI noise power  $P_{\text{NLI}}$  can be written as:

$$P_{\text{NLI}} = G_{\text{NLI}} \cdot B_n \quad (2)$$

where  $G_{\text{NLI}}$  is the PSD of NLI. The above formula assumes that  $G_{\text{NLI}}$  is locally 'white'. This is not true in general, but it is very well verified at the Nyquist limit, especially over the center channel of the WDM comb.

In [13] an approximated but very accurate expression of  $P_{\text{NLI}}$  at the Nyquist limit was provided for the case of lumped (EDFA) amplification:

$$P_{\text{NLI}}^{\text{EDFA}} \approx \left(\frac{2}{3}\right)^3 N_s \gamma^2 L_{\text{eff}} P_{\text{Tx,ch}}^3 \frac{\ln(\pi^2 |\beta_2| L_{\text{eff}} N_{\text{ch}}^2 R_s^2)}{\pi |\beta_2| R_s^3} B_n \quad (3)$$

where  $N_s$  is the number of spans,  $\gamma$  is the fiber nonlinearity coefficient,  $N_{\text{ch}}$  is the number of WDM channels and  $\beta_2$  is fiber dispersion.  $L_{\text{eff}}$  is the effective length, defined as:  $L_{\text{eff}} = [1 - \exp(-2\alpha L_s)] / (2\alpha)$ , with  $\alpha$  the fiber loss coefficient and  $L_s$  the span length.

Not shown in [13], a similar expression can also be found for the case of ideal distributed amplification (DA):

$$P_{\text{NLI}}^{\text{DA}} \approx \left(\frac{2}{3}\right)^3 \gamma^2 L_{\text{tot}} P_{\text{Tx,ch}}^3 \frac{\ln(\pi^2 |\beta_2| L_{\text{tot}} N_{\text{ch}}^2 R_s^2)}{\pi |\beta_2| R_s^3} B_n \quad (4)$$

where  $L_{\text{tot}}$  is the total link length. Though approximations, both Eqs. (3)-(4) asymptotically converge to the exact NLI model prediction as the logarithm argument is increased.

As for  $P_{\text{ASE}}$  in Eq. (1), the standard formulas:

$$P_{\text{ASE}}^{\text{EDFA}} = N_s F (e^{2\alpha L_s} - 1) h \nu B_n \quad (5)$$

and

$$P_{\text{ASE}}^{\text{DA}} = 4\alpha L_{\text{tot}} h \nu K_T B_n \quad (6)$$

can be used, where  $F$  is the EDFA amplifiers noise figure,  $h$  is the Plank's constant,  $\nu$  is the center frequency of the WDM comb and  $K_T \geq 1$  is a constant which is approximately equal to 1.13 for realistic Raman amplification [12].

Regarding the EDFA amplification scenario, the accuracy of performance prediction based on Eqs. (1)-(3) at the Nyquist limit was extensively checked for PM quadrature phase-shift keying (PM-QPSK) in [13]. A more comprehensive test of the NLI model, encompassing PM-BPSK (binary phase-shift keying), PM-QPSK, PM-8QAM and PM-16QAM (quadrature-amplitude modulation with 8 and 16 symbols, respectively), was carried out in [14], [15], addressing also frequency spacings larger than  $R_s$  and three different fiber types. All these tests were performed using simulations based on direct error counting at the receiver. A very good agreement was found throughout. In particular, the model proved accurate for all the tested formats, confirming, as its derivation appears to imply [14], [15], that it should be valid with any coherent format of any cardinality. If so, it can then be used together with the ideally Gaussian constellation which provides the maximum achievable capacity [12], [25].

Note that a first experimental model validation, based on PM-QPSK, was recently presented in [20]. The experiment too showed good agreement with the model, on three different fiber types.

### 3. Optical channel capacity with Gaussian constellation at the Nyquist limit

Resorting to Shannon's formula [25] for the unconstrained additive white-Gaussian-noise (AWGN) channel capacity  $C = \log_2(1 + \text{SNR})$  [bit/s/Hz], where SNR is the ratio between the average signal power and the noise variance at the Rx decision stage, it is then possible to derive a similar formula for the polarization-multiplexed (PM) optical channel:

$$C = 2 \frac{R_s}{\Delta f} \log_2(1 + \text{SNR}) \quad [\text{bit/symbol}] \quad (7)$$

with:

$$\text{SNR} = \frac{B_n}{R_s} \text{OSNR}_{\text{NL}}. \quad (8)$$

The relationship between SNR and  $\text{OSNR}_{\text{NL}}$  assumes matched electrical filtering. Note that since typical Rx adaptive equalizers tend towards matched filtering, this condition is also a realistic one.

Expressing  $\text{OSNR}_{\text{NL}}$  according to Eqs. (1)-(6), we obtained the following expressions of the non-linear optical channel capacity for both the EDFA and DA case:

$$C^{\text{EDFA}} = 2 \log_2 \left( 1 + \frac{G_{T_x}}{N_s (a + b G_{T_x}^3)} \right) \quad (9)$$

$$C^{\text{DA}} = 2 \log_2 \left( 1 + \frac{G_{T_x}}{L_{\text{tot}} (c + d G_{T_x}^3)} \right) \quad (10)$$

where the signal PSD  $G_{T_x} = P_{T_x, \text{ch}}/R_s$  is a sort of "average energy" of the WDM comb and  $a$  (or  $c$ ) and  $b$  (or  $d$ ) are related, respectively, to the linear and nonlinear noise contributions through the following relationships:

$$\begin{aligned} a &= (e^{2\alpha L_s} - 1) F h \nu, & b &= \left(\frac{2}{3}\right)^3 \gamma^2 L_{\text{eff}} \frac{\ln(\pi^2 |\beta_2| L_{\text{eff}} B_{\text{WDM}}^2)}{\pi |\beta_2|} \\ c &= 4\alpha h \nu K_T, & d &= \left(\frac{2}{3}\right)^3 \gamma^2 \frac{\ln(\pi^2 |\beta_2| L_{\text{tot}} B_{\text{WDM}}^2)}{\pi |\beta_2|} \end{aligned} \quad (11)$$

where  $B_{\text{WDM}} = N_{\text{ch}} \cdot R_s$  is the total WDM optical bandwidth.

Eqs.(9)-(11) provide a closed-form capacity limit for the dual-polarization non-linear optical channel with UT, that is a sort of "optical non-linear Shannon-limit". They also emphasize the fact that capacity does not depend on the symbol-rate, as long as the signal PSD and WDM bandwidth remain constant. Capacity decreases as  $B_{\text{WDM}}$  is increased, though weakly due to the logarithm. This behavior is characteristic not only of the PM-Gaussian constellation which yields the ultimate capacity limits, but it can be shown to hold for any PM coherent format with UT. For instance, for PM-QPSK at the Nyquist limit a similar performance invariance vs. the symbol-rate was found in [13], though in terms of BER rather than capacity. A simulative validation was provided too.

In Fig. 1 we plot the capacity limit in bit/symbol (equivalent, at the Nyquist limit, to bit/s/Hz) vs. the launch power per channel. We assume ideal DA with  $K_T = 1$  (Fig. 1a) or EDFA amplification with  $F=5$  dB and  $L_{\text{span}}=100$  km (Fig. 1b). 125 channels at 32 GBaud each are considered, covering a total optical bandwidth  $B_{\text{WDM}}$  of 4 THz (approximately the C band). Each curve refers to a different system length, from 500 to 8000 km for DA and from 100 to 1600 km for EDFA amplification. The fiber is standard single-mode (SSMF) with same parameters as in [12]:  $\gamma = 1.27$  1/W/km,  $\alpha = 0.22$  dB/km,  $\beta_2 = -21.7$  ps<sup>2</sup>/km.

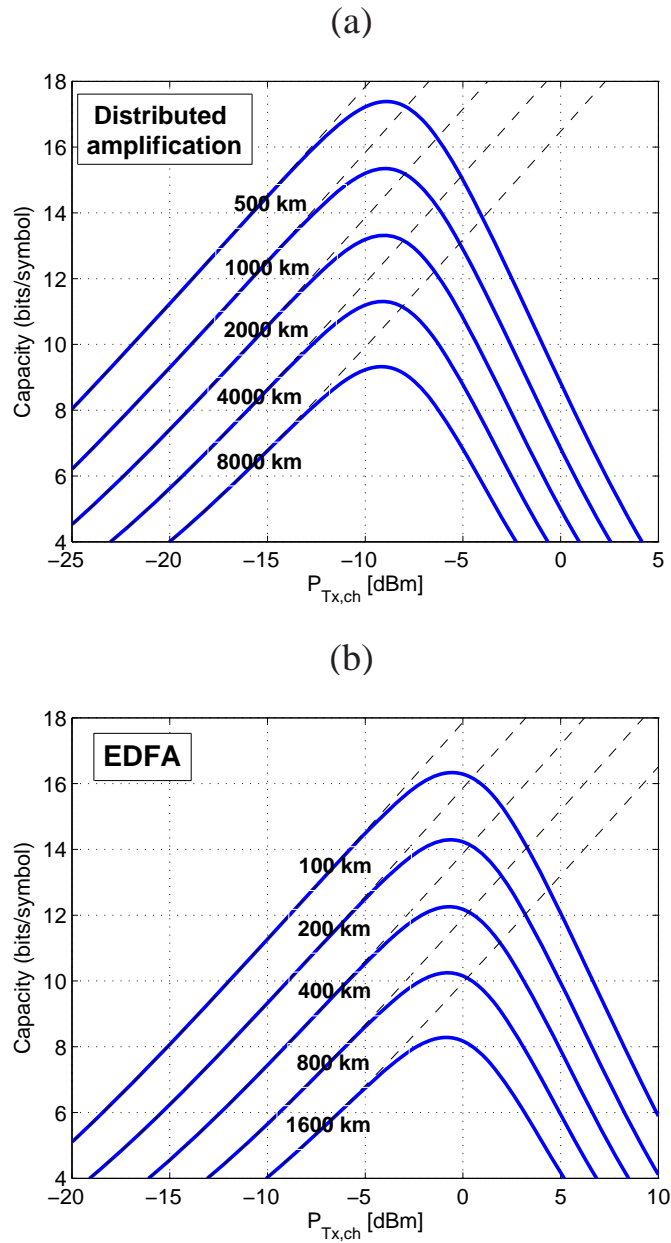


Fig. 1. Capacity limit vs. launch power per channel at different system lengths with ideal distributed-amplification (a) and EDFA amplification with  $F=5$  dB,  $L_S=100$  km (b). Assumptions: UT and PM-Gaussian constellation, 125 channels at 32 GBaud, channel spacing equal to symbol-rate, resulting in a total optical bandwidth of 4 THz. Dashed lines: Shannon limit - Eq. (7). Solid lines: non-linear capacity limit - Eq. (9),(10).

Figure 1 has two distinctive features. First, the peak capacity appears to decrease by about 2 bits/symbol for every doubling of distance. To verify this visual guess, we derived from Eqs. (9)-(11) the expressions of peak capacity for both the EDFA and DA cases:

$$C_{\max}^{\text{EDFA}} = 2\log_2 \left( 1 + \frac{2^{\frac{1}{3}}}{N_s [(e^{2\alpha L_s} - 1) F h \nu]^{\frac{2}{3}} [\gamma^2 L_{\text{eff}} \ln(\pi^2 |\beta_2| L_{\text{eff}} B_{\text{WDM}}^2)]^{\frac{1}{3}}} \right) \quad (12)$$

and

$$C_{\max}^{\text{DA}} = 2\log_2 \left( 1 + \frac{2^{\frac{1}{3}}}{L_{\text{tot}} [4\alpha h \nu K_T]^{\frac{2}{3}} [\gamma^2 \ln(\pi^2 |\beta_2| L_{\text{tot}} B_{\text{WDM}}^2)]^{\frac{1}{3}}} \right) \quad (13)$$

Fixing all other parameters, and neglecting the dependence on  $L_{\text{tot}}$  within the inner logarithmic term in Eq. (13), it is easy to derive approximate laws for the peak capacity which confirm the decrease of about 2 bits/symbol for every doubling of distance for both EDFA and distributed amplification:

$$C_{\max}^{\text{EDFA}} \propto -2\log_2(N_s), \quad C_{\max}^{\text{DA}} \propto -2\log_2(L_{\text{tot}}) \quad (14)$$

Note that the previous relationships hold in general for capacity at any channel power, as can be easily derived from Eqs.(9)-(10).

The other distinctive feature of Fig. 1 is the fact that all maxima occur at approximately the same  $P_{\text{Tx, ch}}$  ( $\simeq -0.9$  dBm for the EDFA case and  $\simeq -9.0$  dBm for distributed amplification), independently of link length. We will further discuss this aspect in Sect. 4. Note also that, as shown in [26,27], the optimum channel power corresponds to the case in which the power of the nonlinear interference is exactly half of the power of the ASE noise. As an example, the values of  $P_{\text{ASE}}$  and  $P_{\text{NLI}}$  corresponding to the optimum launch power of -0.9 dBm in Fig. 1b can be evaluated using Eqs.(3) and (5), obtaining, at 1600 km,  $P_{\text{ASE}} \simeq -18.9$  dBm and  $P_{\text{NLI}} \simeq -21.9$  dBm over a 0.1 nm bandwidth.

Figure 1 appears to be similar to Fig. 3 in [12]. Our values are slightly less than twice those in [12]. The doubling stems from the fact that we assume dual-polarization, whereas [12] assumes single. Also, Eqs. (9)-(10) include cross-polarization interference, which could in part justify values slightly lower than double, together with the fact that [12] used (single-channel) backward propagation non-linear compensation in the receiver simulation.

#### 4. Optical channel capacity for realistic constellations

To obtain capacity estimates for generic PM coherent formats in UT links, we resorted to the standard formulas of capacity over AWGN [21], [25], specific of each format, adapting them to the polarization-multiplexed optical channel. Assuming that all symbols have the same a priori probability, the channel capacity for hard-decision is given by:

$$C^{\text{hard}} = 2 \frac{R_s}{\Delta f} \frac{1}{M} \sum_{a \in X, b \in Y} P_{Y|X}(b|a) \log_2 \frac{P_{Y|X}(b|a)}{P_Y(b)} \quad (15)$$

where  $M$  is the number of constellation points,  $X = \{x_1, \dots, x_M\}$  is the set of possible transmitted symbols,  $Y = \{y_1, \dots, y_M\}$  is set of the output symbols after hard-decision,  $P_{Y|X}(b|a)$  is the probability of receiving the symbol  $b$  when the symbol  $a$  has been transmitted,  $P_Y(b)$  is the probability of receiving the symbol  $b$ .

Similarly, assuming soft-decision, we get:

$$C^{\text{soft}} = 2 \frac{R_s}{\Delta f} \frac{1}{M} \sum_{a \in X} \int p_{Y|X}(y|a) \log_2 \frac{p_{Y|X}(y|a)}{p_Y(y)} \quad (16)$$



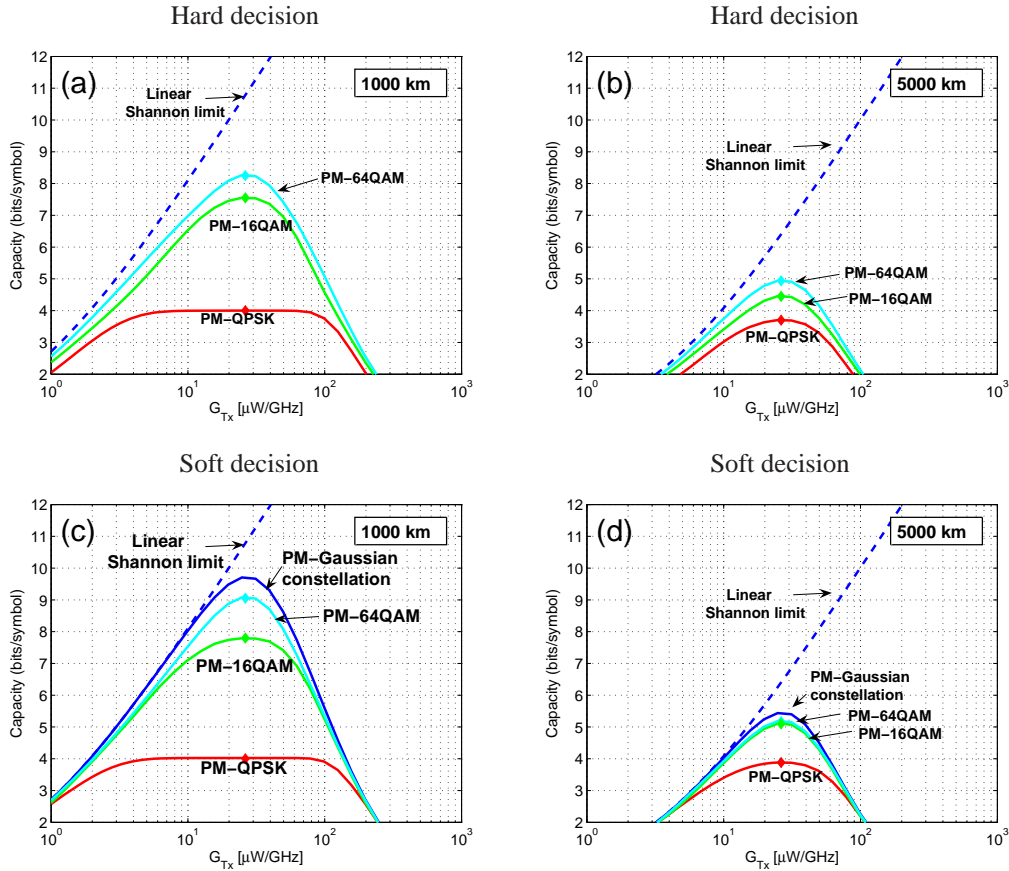


Fig. 2. Capacity vs. launch power spectral density after 1000 km (a-c) and 5000 km (b-d) over SSMF with span length 100 km. WDM transmission over the whole C-band ( $B_{WDM}=4$  THz) at the Nyquist limit (rectangular spectra with spacing  $\Delta f = R_s$ ). Markers: curve maxima.

where  $y$  is the soft value at the output of the channel,  $p_{Y|X}(y|a)$  is the probability density function of the random variable  $y$ ,  $p_Y(y)$ , conditioned to the transmission of the symbol  $a$ .

Assuming transmission over an AWGN channel and using standard information theory results [21], it is possible to evaluate analytically all transition probabilities in Eqs. (15)-(16) in terms of SNR at the receiver. In a PM optical channel, the values of SNR can be derived, through Eq. (8), from the generalized OSNR of Eq. (1). When the channel spacing  $\Delta f$  is equal to the symbol-rate  $R_s$ , the amount of  $P_{NLI}$ , required to estimate the OSNR<sub>NL</sub>, is evaluated using Eqs. (3)-(4). If  $\Delta f > R_s$ ,  $P_{NLI}$  can be obtained by resorting to the integral formula provided in [13–15], solving it by numerical integration.

## 5. Examples of application of the capacity formulas

### 5.1. Terrestrial link with EDFA amplification - Nyquist limit

As an example, in Fig. 2 the values of capacity obtained for PM-QPSK, PM-16QAM and PM-64QAM with both hard and soft decision and EDFA amplification are shown for two distances (1000 and 5000 km) over SSMF fiber. The plateau of bit/symbol reached by PM-QPSK at 1000 km means that, at this link length, capacity is limited by the cardinality of the constellation

rather than by signal degradation. This means that the “asymptotic effect”, caused by the finite number of constellation symbols, occurs largely before the limitation due to non linear effects. PM-16QAM almost reaches its 8 bit/symbol theoretical maximum, while PM-64QAM is significantly limited and falls well short of its ideal 12 bit/s/Hz. The PM-Gaussian constellation is theoretically optimum and therefore it outperforms all other formats. Going to 5000 km, the values of capacity decrease for all formats, as expected, with higher-order modulation formats being far away from their ideal capacity values.

Table 1. Raw (pre-FEC) BER values corresponding to the maximum capacity points (diamond markers in Fig. 2).

	1000 km	5000 km
PM-QPSK	$6 \cdot 10^{-8}$	$9 \cdot 10^{-3}$
PM-16QAM	$7 \cdot 10^{-3}$	$1 \cdot 10^{-1}$
PM-64QAM	$7 \cdot 10^{-2}$	$2 \cdot 10^{-1}$

Notice the somewhat counter-intuitive result, which is found for any fiber length or system parameters, that higher-cardinality constellations potentially deliver a higher net capacity than lower-cardinality ones (though needing more complex FECs to do so). The same result is found in Shannon’s theory for the AWGN channel and the reason why the non-linear UT optical channel behaves similarly is that NLI noise can be approximated as AWGN as well.

One prominent feature of Fig. 2 is that the optimum launch power is independent of link length (for a fixed span length) and is the same for every modulation format (either Gaussian constellation or QAM modulations). In fact, the value of the optimum signal PSD which maximizes the channel capacity, obtained from Eq. (9), is:

$$G_{Tx,opt}^{EDFA} = \left(\frac{a}{2b}\right)^{\frac{1}{3}} = \frac{3}{2^{4/3}} \left(\frac{(e^{2\alpha L_s} - 1)Fh\nu\pi|\beta_2|}{\gamma^2 L_{\text{eff}} \ln(\pi^2|\beta_2|L_{\text{eff}}B_{\text{WDM}}^2)}\right)^{\frac{1}{3}} \quad (17)$$

and clearly the number of spans does not appear in it. A similar formula can be derived for distributed amplification as well, using Eq. (10):

$$G_{Tx,opt}^{DA} = \left(\frac{c}{2d}\right)^{\frac{1}{3}} = \frac{3}{2^{4/3}} \left(\frac{4\alpha L_{\text{tot}}h\nu K_T \pi|\beta_2|}{\gamma^2 L_{\text{tot}} \ln(\pi^2|\beta_2|L_{\text{tot}}B_{\text{WDM}}^2)}\right)^{\frac{1}{3}} \quad (18)$$

Note however that the capacity maximum is reached at very different BER values among formats. It is in fact their high pre-FEC BER values that make PM-16/64QAM capacity substantially lower than ideal. The values of pre-FEC BER corresponding to the maximum capacity points (diamond markers in Fig. 2) are shown in Table 1. Notice that pre-FEC values are obviously hard-decision-based, and therefore they are the same, whether the subsequent FEC is either hard or soft. Using soft-decision FECs, higher values of capacity can be achieved with respect to hard-decision FECs, essentially because soft-FECs need a lower redundancy than hard-FECs to obtain virtually error-free, but the advantage is quite moderate: as an example, at 1000 km the maximum capacity increases from 7.6 to 7.8 bits/symbol for PM-16QAM and from 8.2 to 9 bits/symbol for PM-64QAM.

Note also that the ratio between the lost (hard or soft) capacity and the maximum capacity of a format corresponds to the minimum required ideal (hard or soft) FEC overhead necessary to obtain an arbitrarily low BER [21]. When using soft decision, the loss in capacity is lower, meaning that a lower FEC overhead is required than in the hard decision case. Practical FECs of

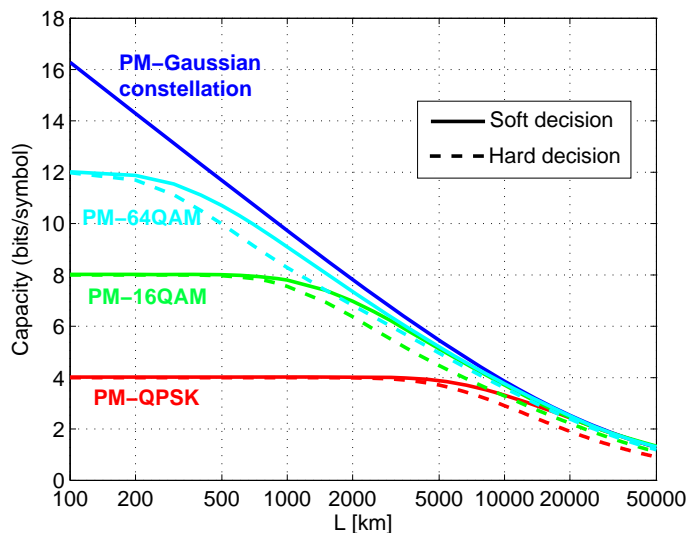


Fig. 3. Maximum capacity vs. transmission distance, over SSMF with span length 100 km and EDFA noise Fig. 5 dB. Solid curves: soft decision. Dashed curved: hard decision. WDM transmission over the whole C-band at the Nyquist limit (total optical bandwidth  $B_{WDM}=4$  THz, symbol-rate spacing, rectangular spectra).

course need higher overheads, although state-of-the-art FECs come rather close to the minimum required overhead.

The dependence of maximum capacity on total link length is plotted in Fig. 3 for both hard and soft decision, assuming C-band transmission at the Nyquist limit. The results of Figs. 3 clearly highlight the trade-off between distance and capacity, in relation to the different modulation formats. Increasing the cardinality of the constellation, a higher capacity can be achieved, but typically over a shorter transmission distance and/or at a higher required FEC complexity. As an example, in Fig. 3, assuming a reference 20% hard-FEC overhead, the system can reach a distance of up to 500 km using PM-64QAM, 2000 km using PM-16QAM and 10000 km using PM-QPSK, approximately.

### 5.2. Terrestrial link with EDFA amplification - 32 Gbaud with 50 GHz spacing

Figure 4 addresses a more realistic case of transmission of 32-Gbaud channels with 50 GHz spacing, where the number of channels was set equal to 11 in order to be able to validate the results through numerical simulations (dots in figure). Capacity was predicted using Eq. (7), together with Eq. (4) in [13]. The latter provides  $P_{NLI}$  when the spacing is different from the symbol-rate, and requires numerical integration. Note that the plateau values of channel capacity in Fig. 4 are lower than ideal due to the loss of spectral efficiency induced by the channel spacing being larger than the symbol-rate ( $R_s/\Delta f = 32/50 = 0.64$ ). The simulation dots were obtained by estimating the capacity from BER values [12], [21] and show a good agreement with the predicted capacity. This confirms the accuracy of the NLI model [13–15] and, as a consequence, of capacity estimation based on it.

Note that, at any given distance the capacity values of Fig. 3 are always larger than those of Fig. 4, which shows that from the viewpoint of maximizing capacity, tighter spectral packing should be pursued: the greater impact of non-linearity is not enough to offset the capacity gain.

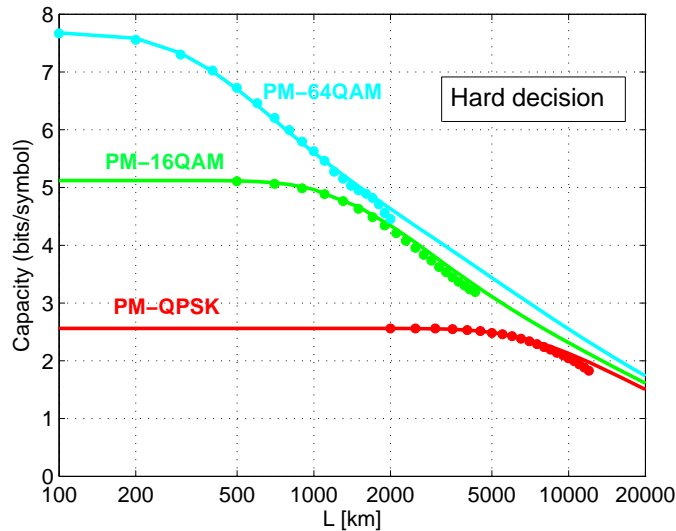


Fig. 4. Maximum hard-decision capacity vs. transmission distance for 11 channels at 32 Gbaud and 50 GHz spacing over SSMF with span length 100 km and EDFA noise figure 5 dB. Solid curves: analytical prediction. Dots: simulations.

### 5.3. Submarine link with EDFA amplification and PSCF fiber - Nyquist limit

In this subsection we analyze the capacity of a submarine link, assuming a typical span length equal to 50 km, with EDFA amplification over pure-silica-core fiber (PSCF). The dependence of maximum capacity on total link length is plotted in Fig. 5 for both hard and soft decision, assuming C-band transmission at the Nyquist limit. The fiber parameters are:  $\gamma = 0.9$  1/W/km,  $\alpha = 0.18$  dB/km,  $\beta_2 = -26.3$  ps<sup>2</sup>/km.

Obviously, decreasing the span length allows to increase the maximum reachable distance for all modulation formats. This plot shows that, potentially, also PM-16QAM could reach ultra-long-haul distances (beyond 8,000 km with 20% hard-FEC overhead) over submarine-like links.

## 6. Conclusion

We have derived simple analytical capacity-limit formulas, based on a recently proposed non-linear propagation model for uncompensated transmission, both with lumped and ideal distributed amplification. We have also shown how to evaluate the capacity of any specific transmission format at the Nyquist limit. The found results are consistent with the simulation results in [12].

Our formulas permit to clearly assess the dependence of capacity on the main link parameters. For instance, from Eqs.(9)-(10) we infer that dispersion improves capacity, whereas the symbol-rate has no effect as long as the transmitted power spectral density and total WDM bandwidth are kept constant.

We have also estimated the capacity of various practical modulation formats with hard and soft-decision, validating the results with simulations. We have shown that the launch power density which maximizes capacity is independent of format and link length (all other parameters fixed). Moreover, resorting to tighter spectral packing appears to improve capacity despite the greater non-linear effects it excites. Finally, we have discussed the optimal distance range of

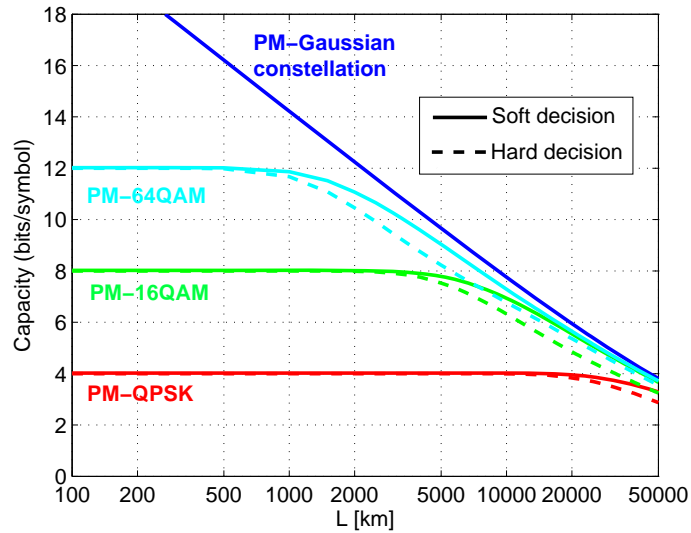


Fig. 5. Maximum capacity vs. transmission distance, over PSCF with span length 50 km and EDFA noise figure 5 dB. Solid curves: soft decision. Dashed curved: hard decision. WDM transmission over the whole C-band at the Nyquist limit (total optical bandwidth  $B_{WDM}=4$  THz, symbol-rate spacing, rectangular spectra).

PM-QPSK, PM-16QAM and PM-64QAM, in terms of delivered capacity with reasonable complexity (20% hard-FEC overhead), assuming EDFA amplification and either 100-km SSMF or 50-km PSCF spans. The obtained results clearly highlighted the trade-off between capacity and reach for each modulation format.

### Acknowledgments

This work was supported by CISCO Systems (SRA contract) and by the EURO-FOS project, a Network of Excellence funded by the European Commission through the 7th ICT-Framework Programme. The simulator OptSim was supplied by RSoft Design Group Inc.